ACEEE

Int. J. on Recent Trends in Engineering and Technology, Vol. 10, No. 2, Jan 2014

A Novel Approach for Edge Detection using Modified ACIES Filtering

P.Siva Priya[1], B.Sarada[1], G.Srinivas[2] and P.Eswar[2]
[1] SVP College of Engineering\ECE, Visakhapatnam, India
Email: priyasrinivas.gs@gmail.com, Sarada.bandi@yahoo.co.in
[2] Gitam University/IT, Visakhapatnam, India
Email: srinivas.gitam@gmail.com, Eswar.patnala@gmail.com

***Abstract*— The most important humiliating attribute of an image is noise, which may become obvious during image capturing, communication or processing and may conceivably be reliant on or sovereign of image. In order to supplement the high- frequency components in this paper we are proposing a new class of filter called ACIES filter which implies spatial filter shape that has a high positive component at the centre. Since restraint of noise can only be achieved by smoothing the image. Sharpening with ACIES filter highlights the fine details of an image and enhances the clarity of the image at the boundaries. Experimental results show that the concert of the proposed ACIES filter is acceptable and Quality of the consequent images is remarkably well even under the strongly noise-corrupted conditions. If the edges in an image can be recognized specifically, then all the objects in the image can be located and basic properties such as region, edge, and contour can be measured. The performance of the proposed approach is measured with image quality metrics such as PSNR, MSE, NAE and NK.**

***Index Terms*— Image Processing, Spatial Filter, Image Sharpening, Image Smoothing, ACIES Filter**

I. INTRODUCTION

The most important humiliating attribute of an image is noise [1, 2] which may become obvious during image capturing, communication or processing and may conceivably be reliant on or sovereign of image. In order to supplement the high-frequency components in this paper we are proposing a new class of filter called ACIES filter which implies spatial filter shape that has a high positive component at the centre. Since restraint of noise can only be achieved by smoothing the image. Sharpening with ACIES filter highlights the fine details of an image and enhances the clarity of the image at the boundaries. Experimental results show that the concert of the proposed ACIES filter is acceptable and Quality of the consequent images is remarkably well even under the strongly noise-corrupted conditions. If the edges in an image can be recognized specifically, then all the objects in the image can be located and basic properties such as region, edge, and contour can be measured.

Edge detection is one of the frequently used applications in image processing and there are quite a few algorithms developed for identifying the boundaries. The most recurrently used operation in image segmentation, image analysis is Edge detection. The boundary between an object and background can be termed as edge. If the edges in an image can be accredited specifically, then all the objects in the image can be positioned and basic properties such as region, edge, and contour can be easily measured.

DOI: 01.IJRTET.10.2.521

The important anticipatory factor in image enhancement is noise. As a result, in image enhancement [3, 4], one must imagine about how firmly the noise effects the image, particularly when the interaction of noise with the visual manifestation of the image.
In order to reduce noise and other unauthentic effects in an image as a consequence of sampling, quantization, communication, during image acquisition are reduced with the help of smoothening. There are several algorithms for image smoothing and sharpening. The design of these algorithms with good performances is often pricey to propose, execute, as well as compute. On the other hand, the effects of the exiting algorithms are not satisfactory.

II. SHARPENING FILTERS

The process of sharpening edges and contours is done in order to protect the idea of clarity and fine details; it must therefore detect edges acceptably and imitate them smoothly and devoid of over-sharpening. Prewitt, Sobel, Laplacian filters [5] are the sharpening filters where convolution of every point in the image is done with two kernels. One kernel has a maximum retort towards the usual vertical direction and the other kernel has a maximum retort towards the horizontal direction [6, 7 and 8].

III. PROPOSED FILTER

Prewitt, Sobel are the first order derivative based edge detection operators to detect the image edges. ACIES is also a first order derivative based edge detection operator performs a 2-Dimensiional spatial gradient measurement on an image. ACIES is a Latin word means edge. Typically it is used to find the approximate absolute gradient [8] magnitude at each point in an input gray scale image. This edge detector uses a pair of 3x3 convolution masks, one estimating the gradient in the x-direction (columns) and the other estimating the gradient in the y-direction (rows). A size of convolution mask is typically much smaller than the actual image. The resultant image is untrained by sliding mask over an area of the input image, changes that pixel's value and then shifts one pixel to the right and continues to the right until it reaches the end of a row. It then starts at the beginning of the next row.

$$\text{Magnitude} = \sqrt{X^2 + Y^2}$$

Characteristically, an estimated magnitude is computed using:

$$|G| = |G_X| + |G_Y|$$

The Direction of angle of the edge is given by:

$$\text{Edge Direction} = \tan^{-1}\left(\frac{X}{Y}\right)$$

The Gx mask highlights the edges in the horizontal direction while the Gy mask highlights the edges in the vertical direction. After taking the magnitude of both, the resulting output detects edges in both directions.

-1	2	2
-2	0	2
-2	-2	1

-1	-2	-2
2	0	-2
2	2	1

Gx= (-Z1-2Z2-2Z3+2Z4-2Z6+2Z7+2Z8+Z9) Gy= (-Z1+2Z2+2Z3-2Z4+2Z6-2Z7-2Z8+Z9)

The formula shows how a particular pixel in the output image would be calculated. The centre of the mask is placed over the pixel which is going to be manipulated in the image.

IV. ACIES FILTER OF 3*3

A. Generalized Formula

Generalized formula is used to generalize the given filter, but the filter can be generalized only by generalizing the equation. So by which we can increase or decrease our filter size according to quality of the image.

If we want to apply 3*3 filter ,then we need to divide the image into 3*3 matrices and then 3*3 ACIES mask is slide over an area of the input image, changes that pixel's value and then shifts one pixel to the right and continues to the right until it reaches the end of a row. It then starts at the beginning of the next row.

V. EXPERIMENTAL RESULTS

This paper analyzes the comparison between proposed ACIES filter and quite a few kinds of standard algorithms including Prewitt, Sobel (Fig [1]). The perception of human of image quality is not adequate. So we require some more image quality metrics [Table I] like Mean Square Error (MSE), Peak Signal to Noise Ratio (PSNR) [Mar86], Normalized Absolute Error (NAE), and Normalized Correlation (NK) [9, 10, 11, and 12] for efficient measurement of image quality. This section presents the simulation results illustrating the performance of the proposed filter. The test image employed here is the true color image; the tables (II) and (III) are obtained by implementing gradient in horizontal x-direction and vertical y direction.

TABLE I. IMAGE QUALITY METRIC FORMULAE

Image Quality Metric	Procedure to Calculate
Peak-Signal to Noise Ratio	$20 \log_{10}(255/MSE)$ Where MSE is Mean Square Error
Mean Square Error	$(1 \div MN) \sum_{J=1}^{M} \sum_{k=1}^{N} [F(X,Y)-F'(X,Y)]^2$ Where M and N are image rows and columns in spatial form
Normalized Absolute Error	$\sum_{J=1}^{M} \sum_{k=1}^{N} \lvert [F(X,Y)-F'(X,Y)] \rvert / \sum^{M} \sum_{J=1}^{N} \lvert F(X,Y) \rvert$ Where M and N are image rows and columns in spatial form
Normalized Correlation	$\sum_{J=1}^{M} \sum_{k=1}^{N} \lvert [F(X,Y)*F'(X,Y)] \rvert / \sum^{M} \sum_{J=1}^{N} \lvert F(X,Y) \rvert^2$ Where M and N are image rows and columns in spatial form

The mean square error (MSE) is the measure of difference between actual and estimated value of the quantity. Larger the value of MSE implies poor quality (Fig [3], [7]) of the image [David Bethel]. The most familiar image quality metric is PSNR. If PSNR value is high then the difference between the original image and reconstructed image will be small (Fig [2], [6]). The quality of the image increases with decrease in the value of NAE (Fig [4], [8]), Higher the value of NAE means the quality of the image lower. NK (Fig [5], [9]) is the measure of calculating the degree of resemblance between two objects. This paper exploits MATLAB tools to assess these algorithms with image quality metrics. (Images are from Imageprocessingplace.com).

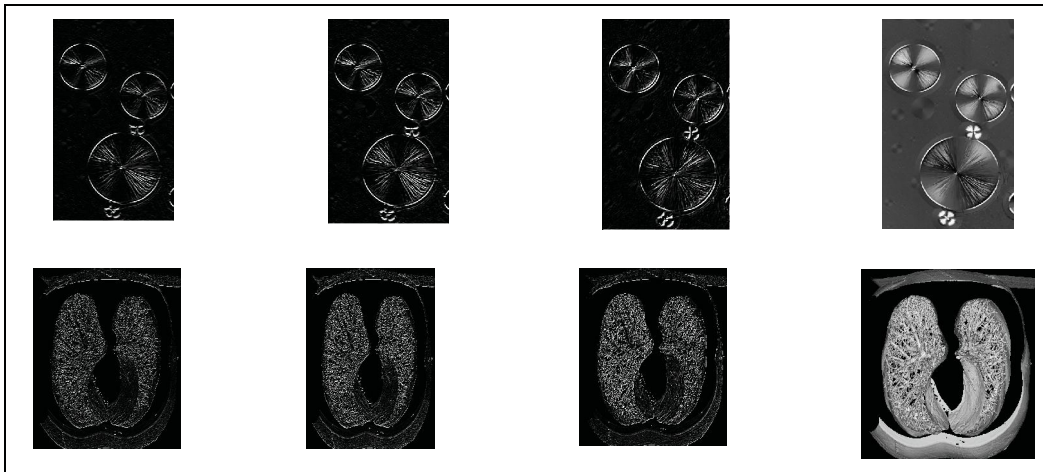

Prewitt Filter	Sobel Filter	Acies Filter	Original Image

Figure 1. Comparison between Prewitt, Sobel,and Acies filters

TABLE II. COMPARISON INTERMS OF PSNR, MSE, NAE AND NK BETWEEN PREWITT, SOBEL AND ACIES

Sno	Image	PSNR			MSE			NAE			Nk		
		Prewitt	Sobel	Acies	Prewitt	Sobel	Acies	Prewitt	Sobel	Acies	Prewitt	Sobel	Acies
1	Cktboard.tif	4.98	5.07	5.13	2.06	2.02	1.94	0.85	0.839	0.828	0.199	0.242	0.28
2	Circuit.tif	5.76	5.9	6.06	1.72	1.66	1.54	0.91	0.89	0.87	0.1	0.14	0.18
3	Fractal-iris.tif	8.49	8.52	8.54	0.92	0.913	0.905	0.92	0.91	0.9	0.19	0.24	0.26
4	Characters Test Pattern.tif	1.4	1.4	1.4	4.70	4.70	4.68	0.98	0.98	0.98	0.03	0.03	0.035
5	CTskull.tif	5.73	5.84	5.83	1.73	1.62	1.65	0.938	0.9	0.92	0.0697	0.092	0.094
6	Letter_T.tif	10.61	10.61	10.63	0.563	0.564	0.568	1	1	0.99	0.0245	0.025	0.044
7	Mri_of_Knee_Univ_Mich	4.2	4.28	4.32	2.47	2.42	2.386	0.89	0.88	0.88	0.116	0.15	0.17
8	Mri_Spine1_vandy	9.5	9.63	9.69	0.729	0.706	0.639	0.92	0.89	0.88	0.08	0.1	0.14
9	Pentagon.tif	5.8	5.96	6.03	1.70	1.64	1.5833	0.9	0.88	0.87	0.0989	0.134	0.15
10	Mexico-plate.tif	10.56	10.56	10.61	0.570	0.570	0.552	0.89	0.88	0.88	0.178	0.21	0.21
11	Organic Super Conductor.tif	9.24	9.314	9.344	0.774	0.761	0.748	0.85	0.88	0.86	0.1457	0.218	0.3
12	Lung.tif	7.95	7.99	7.99	1.04	1.03	1.031	0.87	0.86	0.86	0.19	0.24	0.3
13	Nickel oxide thin film	6.51	6.5	6.5	1.45	1.47	1.48	0.86	0.86	0.86	0.249	0.3	0.26
14	Taxol-anti-cancer-agent	10.21	10.19	10.32	6.19	0.622	0.637	0.92	0.91	0.9	0.18	0.22	0.22
15	HeadCt-Vandy.tif	6.74	6.82	6.87	1.377	1.35	1.308	0.94	0.93	0.92	0.086	0.1	0.129
16	Bottles	7.09	7.23	7.26	1.26	1.23	1.211	0.92	0.9	0.88	0.069	0.092	0.149
17	Wirebond_mask.tif	5.45	5.45	5.87	1.85	1.85	1.849	1.01	1.01	1	0.0329	0.034	0.038
18	Van_Original.tif	6.3	6.39	6.47	1.52	1.49	1.44	0.91	0.9	0.88	0.1	0.129	0.13
19	Kidney_original.tif	6.81	6.97	7.09	1.35	1.30	1.234	0.92	0.89	0.88	0.08	0.1	0.136
20	Chest-xray-vandy.tif	4	4.06	4.12	2.58	2.57	2.46	0.96	0.95	0.94	0.3445	0.045	0.056
21	Lens-perceptics.tif	6.66	6.71	7.43	1.40	1.38	1.076	0.97	0.96	0.85	0.03	0.04	0.145
22	Noisy_rectangle	53.7	53.73	53.73	0.27	0.2750	0.2750	1.004	1	1	0.0074	0.008	0.01
23	Penny.tif	50.78	50.78	50.75	0.5426	0.5426	0.5426	0.9939	0.994	1	0.0115	0.012	0.018
24	Lines.tif	6.937	6.937	6.937	1.31	0.3163	1.31	1.0027	1.003	1.003	0.0048	0.005	0.146
25	Marion_airport	8.04	8.18	0.955	1.02	0.986	0.952	0.1365	0.866	0.84	0.8886	0.18	0.27
26	star.tif	1.938	5.319	5.235	5.256	1.9107	1.947	0.9722	0.966	0.978	0.0538	0.728	0.096
27	Calculator.tif	10.06	10.13	10.31	0.64	0.631	0.615	0.911	0.896	0.87	0.1534	0.185	0.277
28	Building_original	4.788	4.84	4.878	2.15	2.13	2.14	0.9	0.895	0.895	0.09	0.117	0.147
29	Skull.tif	10.52	10.62	10.53	0.575	0.562	0.547	0.91	0.9	0.921	0.0839	0.111	0.127
30	Brain.tif	5.7	5.76	5.83	1.75	1.7248	1.67	0.96	0.949	0.94	0.0381	0.049	0.066
31	Brain.thumb.tif	10.03	9.92	9.6	0.644	0.66	0.716	0.99	1.008	1.042	0.177	0.233	0.323
32	Pills.tif	4.81	4.907	5.124	2.14	2.100	2.034	0.93	0.925	0.899	0.0636	0.083	0.118

33	Region.tif	4.52	4.528	4.53	2.3	2.3	2.29	0.998	0.998	0.998	0.0322	0.032	0.038
34	Rose1024.tif	10.45	10.6	10.66	0.585	0.566	0.546	0.9152	0.89	0.88	0.0665	0.091	0.124
35	Tungsten_flmt.tiff	7.3893	7.52	7.52	1.18	1.15	1.100	0.9125	0.89	0.885	0.1045	0.14	0.217
36	u.tif	7.045	7.04	7.045	1.28	1.28	1.28	1	1	1.004	0.0128	0.013	0.026
37	Utk.tif	17.15	17.1	17.16	0.125	0.126	0.125	1.01	1.022	1.004	0.14	0.148	0.236
38	Turbine.tif	5.49	5.68	6.041	1.83	1.755	1.544	0.92	0.892	0.835	0.076	0.106	0.18
39	Cholesterol.tif	8.32	7.99	7.909	0.956	1.031	0.969	0.865	0.916	0.928	0.3327	0.416	0.489
40	Cameraman.tif	5.997	6.016	6.019	1.64	1.6272	1.6264	0.9377	0.93	0.93	0.0955	0.122	0.17

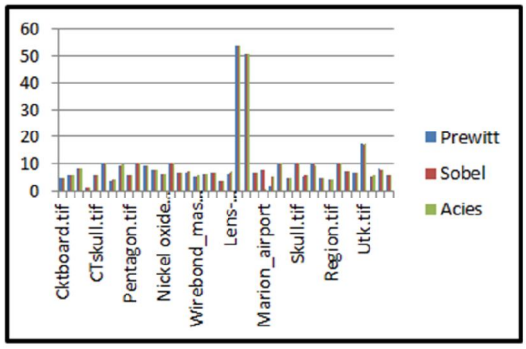

Figure 2. Comparison Interms of PSNR

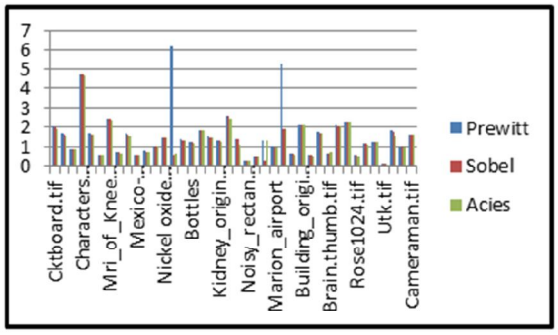

Figure 3. Comparison Interms of MSE

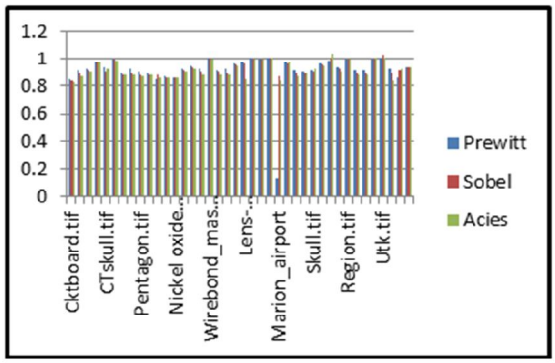

Figure 4. Comparison Interms of NAE

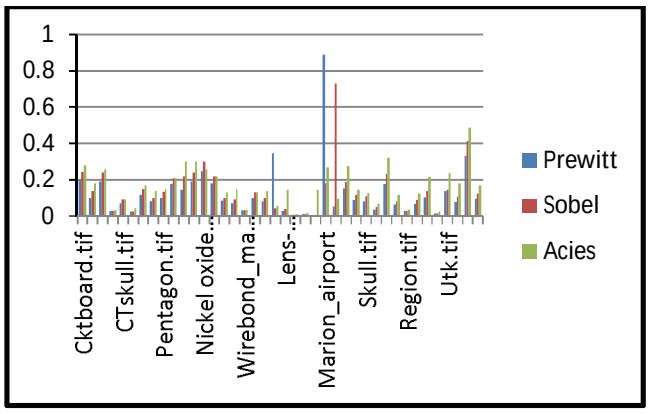

Figure 5. Comparison Interms of Nk

TABLE III. COMPARISON INTERMS OF PSNR, MSE, NAE AND NK BETWEEN PREWITT, SOBEL AND TRANSPOSE OF ACIES

Sno	Image	PSNR			MSE			NAE			Nk		
		Prewitt	Sobel	Acies	Prewitt	Sobel	Acies	Prewitt	Sobel	Acies	Prewitt	Sobel	Acies
1	Cktboard.tif	4.98	5.07	5.198	2.06	2.02	1.99	0.85	0.839	0.818	0.199	0.242	0.329
2	Circuit.tif	5.76	5.9	6.248	1.72	1.66	1.61	0.91	0.89	0.844	0.1	0.14	0.237
3	Fractal-iris.tif	8.49	8.52	8.56	0.92	0.913	0.90	0.92	0.91	0.903	0.19	0.24	0.317
4	Characters Test Pattern.tif	1.4	1.4	1.42	4.70	4.70	4.70	0.98	0.98	0.98	0.03	0.03	0.041
5	CTskull.tif	5.73	5.84	5.94	1.73	1.62	1.69	0.938	0.9	0.908	0.0697	0.092	0.127
6	Letter_T.tif	10.61	10.61	10.58	0.563	0.564	0.562	1	1	1.006	0.0245	0.025	0.045
7	Mri_of_Knee_Univ_Mich	4.2	4.28	4.354	2.47	2.42	2.40	0.89	0.88	0.882	0.116	0.15	0.227
8	Mri_Spine1_vandy	9.5	9.63	10.07	0.729	0.706	0.698	0.92	0.89	0.84	0.08	0.1	0.224
9	Pentagon.tif	5.8	5.96	6.13	1.70	1.64	1.62	0.9	0.88	0.86	0.0989	0.134	0.187
10	Mexico-plate.tif	10.56	10.56	10.7	0.570	0.570	0.564	0.89	0.88	0.87	0.178	0.21	0.247
11	Organic Super conductor.tif	9.24	9.314	9.39	0.774	0.761	0.752	0.85	0.88	0.86	0.1457	0.218	0.311
12	Lung.tif	7.95	7.99	7.99	1.04	1.03	1.03	0.87	0.86	0.864	0.19	0.24	0.313
13	Nickel oxide thin film	6.51	6.5	6.419	1.45	1.47	1.45	0.86	0.86	0.88	0.249	0.3	0.385
14	Taxol-anti-cancer-agent	10.21	10.19	10.08	6.19	0.622	0.603	0.92	0.91	0.917	0.18	0.22	0.284
15	HeadCt-Vandy.tif	6.74	6.82	6.96	1.377	1.35	1.33	0.94	0.93	0.904	0.086	0.1	0.167
16	Bottles	7.09	7.23	7.298	1.26	1.23	1.21	0.92	0.9	0.868	0.069	0.092	0.198
17	Wirebond_mask.tif	5.45	5.45	5.46	1.85	1.85	1.83	1.01	1.01	1.014	0.0329	0.034	0.044
18	Van_Original.tif	6.3	6.39	6.54	1.52	1.49	1.46	0.91	0.9	0.873	0.1	0.129	0.152
19	Kidney_original.tif	6.81	6.97	7.217	1.35	1.30	1.26	0.92	0.89	0.857	0.08	0.1	0.169
20	Chest-xray-vandy.tif	4	4.06	4.221	2.58	2.57	2.513	0.96	0.95	0.935	0.3445	0.045	0.073
21	Lens-perceptics.tif	6.66	6.71	7.81	1.40	1.38	1.17	0.97	0.96	0.8	0.03	0.04	0.239
22	Noisy_rectangle	53.7	53.7	53.7	0.27	0.275	0.275	1.004	1	1	0.007	0.00	0.01

			3	3		0	0				4	8	
23	Penny.tif	50.78	50.78	50.78	0.5426	0.5426	0.5460	0.9939	0.994	0.994	0.0115	0.012	0.018
24	Lines.tif	6.937	6.937	6.93	1.31	0.3163	1.316	1.0027	1.003	1	0.0048	0.005	0.146
25	Marion_airport	8.04	8.18	8.34	1.02	0.986	8.327	0.1365	0.866	0.838	0.8886	0.18	0.273
26	star.tif	1.938	5.319	5.23	5.256	1.9107	1.947	0.9722	0.966	0.978	0.0538	0.728	0.099
27	Calculator.tif	10.06	10.13	10.24	0.64	0.631	0.6051	0.911	0.896	0.875	0.1534	0.185	0.259
28	Building_original	4.788	4.84	4.81	2.15	2.13	2.114	0.9	0.895	0.901	0.09	0.117	0.133
29	Skull.tif	10.52	10.62	10.74	0.575	0.562	0.574	0.91	0.9	0.886	0.0839	0.111	0.146
30	Brain.tif	5.7	5.76	5.89	1.75	1.7248	1.6982	0.96	0.949	0.932	0.0381	0.049	0.068
31	Brain.thumb.tif	10.03	9.92	9.58	0.644	0.66	.0712	0.99	1.008	1.03	0.177	0.233	0.362
32	Pills.tif	4.81	4.907	5.046	2.14	2.100	1.998	0.93	0.925	0.906	0.0636	0.083	0.107
33	Region.tif	4.52	4.528	4.53	2.3	2.3	2.290	0.998	0.998	0.997	0.0322	0.032	0.038
34	Rose1024.tif	10.45	10.6	10.78	0.585	0.566	0.557	0.9152	0.89	0.86	0.0665	0.091	0.13
35	Tungsten_flmt.tiff	7.3893	7.52	7.71	1.18	1.15	1.149	0.9125	0.89	0.858	0.1045	0.14	0.241
36	u.tif	7.045	7.04	7.04	1.28	1.28	1.284	1	1	1.004	0.0128	0.013	0.026
37	Utk.tif	17.15	17.1	17.13	0.125	0.126	0.1248	1.01	1.022	1.01	0.14	0.148	0.234
38	Turbine.tif	5.49	5.68	6.244	1.83	1.755	1.618	0.92	0.892	0.8	0.076	0.106	0.205
39	Cholesterol.tif	8.32	7.99	8.266	0.956	1.031	1.0524	0.865	0.916	0.872	0.3327	0.416	0.449
40	Cameraman.tif	5.997	6.016	6.018	1.64	1.6272	1.6264	0.9377	0.93	0.93	0.0955	0.122	0.17

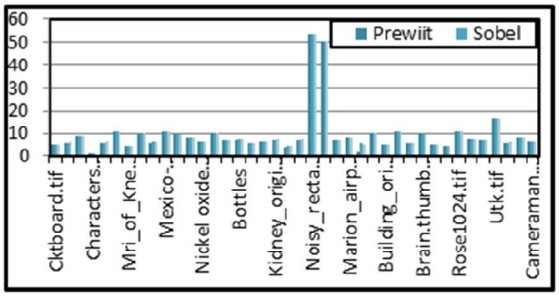

Figure 6. Comparison Interms of PSNR

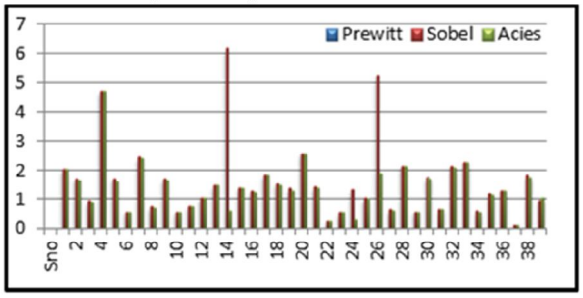

Figure 7. Comparison Interms of MSE

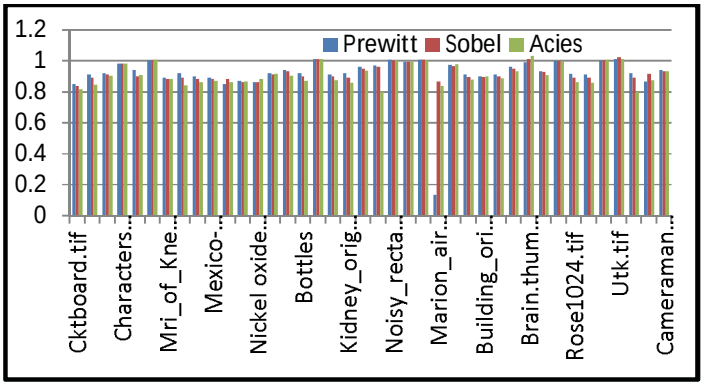

Figure 8. Comparison Interms of NAE

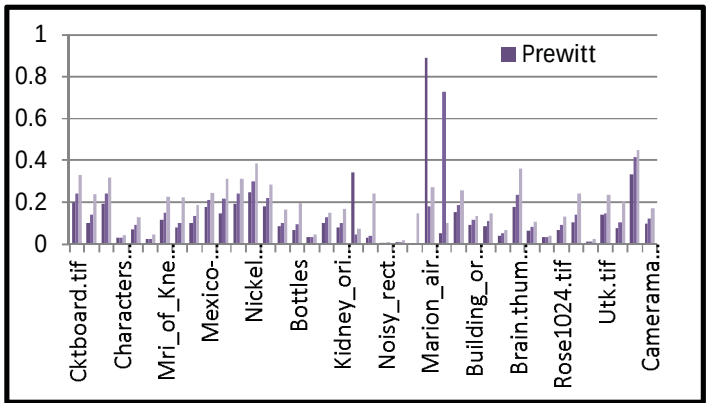

Figure 9. Comparison Interms of Nk

VI. Conclusion

In this attempt we proposed a novel approach for edge detection that can be done by using proposed ACIES filter. The edge detection can be applied in many areas like satellite image enhancement, medical diagnostics, etc. The trialing and simulations with real images have shown that the filter is proficient than the existing filters. In this paper, we have compared Prewitt and Sobel techniques for edge detection in image processing with the proposed technique. We applied various image processing metrics such as MSE, PSNR, NAE and Nk in this assessment. We have generated the enviable code for these new filters and also formed the obligatory strategies of comparisons between these ACIES filters and the existing ones.

References

[1] An Image-Enhancement System Based on Noise Estimation Fabrizio Russo, *Senior Member, IEEE*, IEEE TRANSACTIONS ON INSTRUMENTATION AND MEASUREMENT, VOL. 56, NO. 4, AUGUST 2007.

[2] Gradient Estimation Using Wide Support Operators Hakan Guray Senel, *Member, IEEE*, IEEE TRANSACTIONS ON IMAGE PROCESSING, VOL. 18, NO. 4, APRIL 2009

[3] Gaussian-Based Edge-Detection Methods—A Survey Mitra Basu, *Senior Member, IEEE*, IEEE TRANSACTIONS ON SYSTEMS, MAN, AND CYBERNETICS—PART C: APPLICATIONS AND REVIEWS, VOL. 32, NO. 3, AUGUST 2002

[4] Gray-Scale Image Enhancement as an Automatic Process Driven by Evolution, Cristian Munteanu and Agostinho Rosa, IEEE TRANSACTIONS ON SYSTEMS, MAN, AND CYBERNETICS—PART B: CYBERNETICS, VOL. 34, NO. 2, APRIL 2004

[5] Edge Detection Techniques: Evaluations and Comparisons Ehsan Nadernejad, Applied Mathematical Sciences, Vol. 2, 2008, no. 31, 1507 – 1520.

[6] D.Marr and E. Hildreth, Theory of Edge Detection(London, 1980).

[7] Q.H.Zhang, S Gao and T.D.Bui, Edge detection models, Lecture notes in computer science,32(4), 2005, 133-140.

[8] L.P.Han and W.B. Yin. An Effective Adaptive Filter Scale Adjustment Edge Detection Method. (China, T singhua University 1997).
[9] Z. Wang and A. C. Bovik, Modern Image Quality Assessment, Morgan & Claypool Publishers, 2006.
[10] Ahmet M. Eskicioglu, Paul S. Fisher, "Image Quality Measures and Their Performance" IEEE Transactions on Communication, Vol. 43, No. 12, pp. 2959-2965, December 1995.
[11] Zhou Wang, Alan C. Bovik , "A Universal Image Quality Index", IEEE Signal Processing Letters, Vol. 9, No. 3, pp. 81-84, March 2002.
[12] Ahmet M. Eskicioglu, Paul S. Fisher, "Image Quality Measures and Their Performance" IEEE Transactions on Communication, Vol. 43, No. 12, pp. 2959-2965, December 1995.